IOPscience iopscience.iop.org

Home Search Collections Journals About Contact us My IOPscience

Studies of the ferroelectric domain configuration and polarization of rhombohedral PZT ceramics

This article has been downloaded from IOPscience. Please scroll down to see the full text article.

2000 J. Phys.: Condens. Matter 12 323

(http://iopscience.iop.org/0953-8984/12/3/311)

View the table of contents for this issue, or go to the journal homepage for more

Download details:
IP Address: 171.66.16.218
The article was downloaded on 15/05/2010 at 19:32

Please note that terms and conditions apply.

J. Phys.: Condens. Matter **12** (2000) 323–337. Printed in the UK PII: S0953-8984(00)04579-3

Studies of the ferroelectric domain configuration and polarization of rhombohedral PZT ceramics

J Ricote†, R W Whatmore and D J Barber

School of Industrial and Manufacturing Science, Cranfield University, Cranfield, Bedfordshire MK43 0AL, UK

Received 26 May 1999, in final form 27 September 1999

Abstract. The character of the ferroelectric domains in lead zirconate titanate ($PbZr_{1-x}Ti_xO_3$—PZT) ceramics has been studied using transmission electron microscopy (TEM) for compositions right across the rhombohedral phase ($x = 0.06$ to $x = 0.45$). The polarization hysteresis has also been determined for the same specimens and it has been demonstrated that the compositions between $x = 0.12$ and $x = 0.40$ show double hysteresis loops. It is shown that the occurrence of domain walls which do not correspond exactly to crystallographic planes produces generalized wedge-shaped domains, instead of the typical bands of parallel-sided domains reported in most ferroelectrics. A systematic variation in the arrangement of the domain walls as the composition progresses across the rhombohedral region is reported for the first time. This result is related to the occurrence of double hysteresis loops for these compositions. The role of oxygen octahedral tilts of the low temperature rhombohedral phase in the formation of the domains and in the hysteresis behaviour is discussed.

1. Introduction

Ferroelectric materials are widely used in applications ranging from piezoelectric [1] through pyroelectric [2] to electro-optic devices [3]. One of the most important properties of ferroelectric crystals is that they develop a spontaneous polarization for temperatures below the structural paraelectric–ferroelectric transition marked by the Curie temperature. Crystals develop dipolar domains in order to minimize the charge electrostatic energy associated with this transition. Interest in the study of the ferroelectric domain configurations arises from the fact that they have been shown as a determinant factor of the properties of ferroelectric materials, frequently associated with the grain size [4]. Although ferroelectric domains have been extensively studied for the important ferroelectric composition of lead zirconate titanate (PZT) within the tetragonal phase, the rhombohedral compositions have received little attention, regardless of their interesting structural and physical properties.

A phenomenon which seems to be related to the configuration of ferroelectric domains, and which is present in rhombohedral PZT, is the constriction of the polarization. One of the well known properties of ferroelectrics is the polarization–field (P–E) hysteresis loop. Some ferroelectric materials return to an unpolarized or partially polarized state on field removal, and as a consequence, they show peculiar propeller-shaped hysteresis loops, also called double hysteresis loops. An electrically induced paraelectric–ferroelectric first-order transition, as

† Present address: Instituto de Ciencia de Materiales de Madrid, CSIC, Cantoblanco, 28049 Madrid, Spain.

0953-8984/00/030323+15$30.00 © 2000 IOP Publishing Ltd

found in $BaTiO_3$ crystals above the Curie point, or an induced antiferroelectric–ferroelectric transition, as in $PbZrO_3$, will also result in a similar double-loop behaviour [5]. This has been observed for $BaTiO_3$ [6], $(Pa, Ca)TiO_3$ [7] and the rhombohedral phase of lead zirconate titanate PZT [8]. Except for the $(Pa, Ca)TiO_3$ ceramics, whose dielectric behaviour has been attributed to phase separation, the mechanism suggested to account for the double-loop character, (also called constriction of the hysteresis loops) is an ageing process [9, 10] related to ferroelectric domains. Domain walls move when an electric field is applied, producing the growth of those domains whose dipole directions are the closest to the direction of the applied field. The result is a domain configuration with a net polarization. Usually, when the electric field is removed, the domain walls do not go back to their original positions, resulting in some remanent polarization. However, in the so-called constrained state, domains recover their original configuration on removal of the bias, i.e., to give a zero, or reduced, net polarization. This behaviour has been reported in aged specimens: after cooling from the Curie temperature, normal hysteresis loops are observed, but within hours the constriction of the polarization is developed [6].

Various mechanisms have been proposed in order to explain this phenomenon [11]. Some works have suggested that defects segregated in the crystal can occupy energetically preferred sites in the lattice and then form anisotropic centres which favour a certain direction for the spontaneous polarization. Another possibility is that crystal defects diffuse with time into the domain walls and pin their positions [6, 11]. However, some studies have shown a correlation between changes in the domain patterns and ageing in $BaTiO_3$ [9, 12]. They suggest that when time elapses domain walls move to relieve the residual stresses of the ferroelectric transition or simply to reach more stable positions. The application of an electric field to this stabilized domain configuration would result in the recovery of the original domain configuration on removal of the field.

Dai *et al* [8] have studied extensively the rhombohedral phase of PZT, and reported the progressive appearance of double-hysteresis loops in this phase with increasing Ti content. This effect becomes less pronounced for compositions in the proximity of the rhombohedral–tetragonal morphotropic phase boundary, i.e., at 45% Ti. Dai *et al* suggest that in this particular case, the constriction of the polarization may be due to a disruption of the long-range polar order by random local strains caused by the development of rotations of the octahedral cages of oxygen ions. The electric field would partially align the polar moments, but it would have no effect on the octahedral strains that are affecting the long-range order. Therefore, on removal of the bias, the long-range order would be lost again, and no net polarization would be retained. However, this is a local situation inside the crystal, possibly inside an individual ferroelectric domain. In order to fully explain the overall properties of the grain, it is necessary to study the evolution of the domain configuration as a whole. In the present work we have analysed the characteristics of the domain patterns, in order to give a new insight into this behaviour. A description of the method employed to characterize the ferroelectric domains is given in the next section.

2. Study of ferroelectric domains by TEM in the rhombohedral phase

TEM studies of ferroelectric domains have mainly concerned materials with tetragonal structure, e.g., $BaTiO_3$ [13, 14], modified $PbTiO_3$ [15, 16] and the tetragonal phase of PZT [17, 18]. Very little has been published on the study of rhombohedral phases [19]. The nature of the domain walls, which in fact are twinning planes, varies with the crystal structure. Domain walls can only arise along planes where the conditions of mechanical compatibility are satisfied, i.e., the spontaneous deformation of two neighbouring domains fits each other.

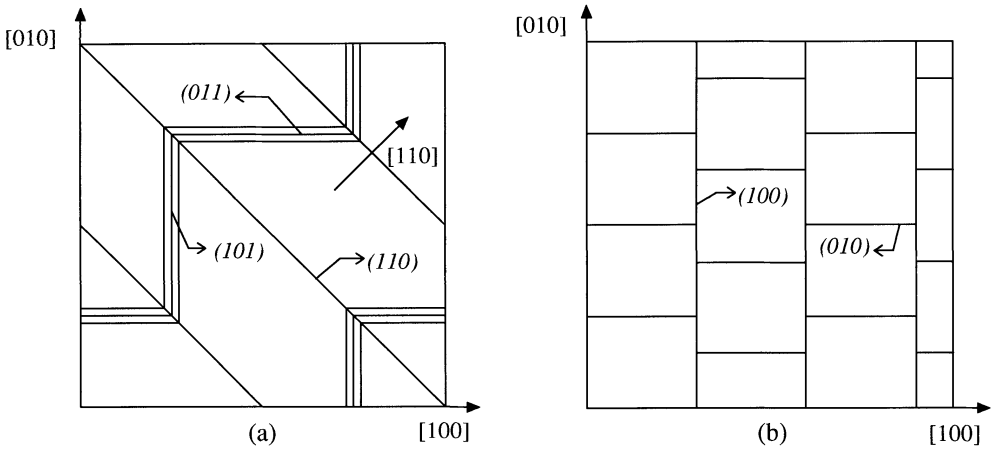

Figure 1. Schematic diagram of ferroelectric domain walls viewed along [001]. (a) {110}-type walls. (b) {100}-type walls.

The orientations of the permissible domain walls can be predicted for the various pseudo-cubic ferroelectric phases of the perovskite structure [20].

For the tetragonal phase, an electric dipole is generated in one of the ⟨100⟩ directions, associated with the displacement of cations along that direction to give a tetragonal unit cell. The rotation of the polarization vector from one domain to the next can only be 90° or 180°. The permissible uncharged walls, i.e., with a head-to-tail arrangement of the dipoles, correspond to {110} planes for the 90° domains, and any plane parallel to the polarization vector for the 180° type.

The polarization vector for the rhombohedral phase is ⟨111⟩†. The rotation between neighbouring domains depends on the cell angle α. For PZT, the rhombohedral angle α equals 91°, and the possible types of domain can be calculated as 109°, 71° and 180°. The orientation of the permissible uncharged walls is {110} for 109°, {001} for 71° and any plane parallel to the polarization vector for 180° domains.

Arlt and Sasko studied the spatial configuration of domains with {110}-type walls and proposed possible models [21, 22]. In polycrystalline materials, two twinning structures are possible which reduce the stress associated with the transition to the ferroelectric phase: sets of simple two-dimensional lamellar twins or complex three-dimensional bands of twins [21]. For the latter, a spatial arrangement of the domain walls has been proposed [22] to fit the observed herringbone-like pattern observed in etched ceramics: long bands traversed by zigzag lines. In the case of characterization by TEM, we only observe the projections of these structures. Figures 1 and 2 show the projected lines of ferroelectric domain walls on two different planes, corresponding to the observation of grains along the main zone axes [001] and [0$\bar{1}$1]. For the sake of clarity, {110} and {100} types of wall are drawn separately, although in reality they can appear in the same locality or even superimposed. Those walls which are not perpendicular to the projection plane, i.e. not parallel to the electron beam, will show a diffraction contrast pattern of fringes in the TEM, which are represented in the diagrams by three closely spaced, parallel lines. These figures can be used as a guide to interpret the TEM micrographs and identify the types of domain wall present in them.

† Miller indices will be assigned on the basis of the pseudo-cubic ≈4 Å unit cell.

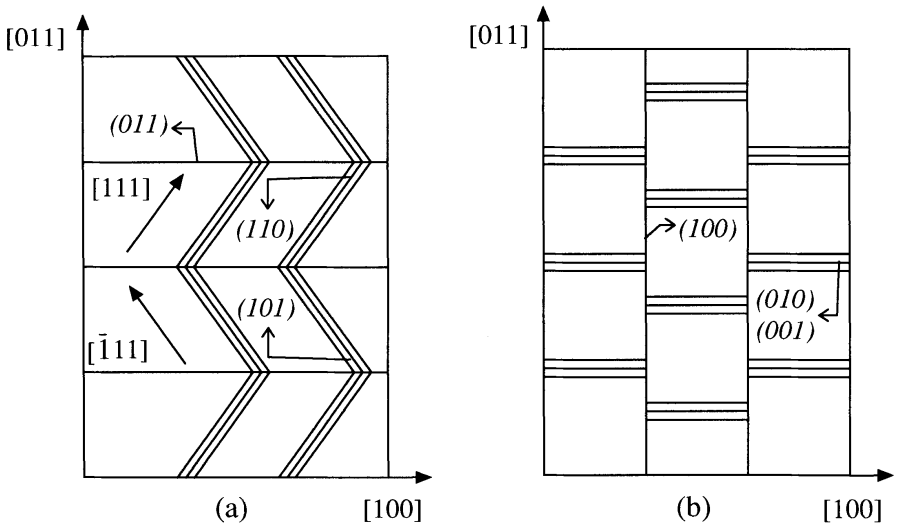

Figure 2. Schematic diagram of ferroelectric domain walls viewed along [0$\bar{1}$1]. (a) {110}-type walls. (b) {100}-type walls.

Electron diffraction patterns taken across a twin plane parallel to the electron beam exhibit the splitting of the spots in a reciprocal space direction which is perpendicular to the domain walls [23]. The magnitude of the splitting increases with the distance from the centre of the pattern. However, for twin planes inclined to the electron beam, the visibility of the split spots can be strongly affected by anomalous absorption [24]. All these features will be considered in the analysis of the various domain walls in this study.

3. Materials and experimental procedure

Ceramics of composition $Pb(Zr_{1-x}Ti_x)O_3$, with $x = 0.06$ (PZT06), 0.12 (PZT12), 0.40 (PZT40) and 0.45 (PZT45), were made from powder prepared by a conventional mixed oxide method, pressed into pellets and sintered at 1573 K for 5 h.

Silver paint electrodes were applied to the largest surfaces of disclike specimens. Polarization against electric field (P–E) curves were obtained with a computer-controlled Sawyer-Tower circuit (Radiant Technologies RT66A unit), equipped with a high voltage interface, which permitted the application of electric fields close to saturation. An initial triangular shaped pulse is used to pole the sample and, after 1 s approximately, another triangular pulse is applied to measure the hysteresis loop. During that intermediate second the remanent polarization decreases both due to the retention characteristics of the sample and its non-infinite resistivity. This results in loops that are usually not closed.

Transmission electron microscopy (TEM) specimens were prepared from 3 mm ceramic discs, which were either mechanically polished to 200 μm thickness and then dimpled in the centre of the disc to $\sim$20 μm, or simply polished to $\sim$20 μm and mounted onto copper '7HEX' (Pelco) TEM grids. This was followed by further thinning to electron transparency by Ar^+ ion milling at 5 kV. Although special care was taken during the preparation of TEM samples, using a low beam incidence angle (7°) and a cooling stage during the ion milling process, a secondary polycrystalline phase developed at the edges of the samples during the final stages of the processing. Traces of the diffraction rings corresponding to this phase can be seen in

the electron diffraction patterns. For the TEM studies we used a Philips CM20 microscope working at 200 kV.

4. Experimental results

Figure 3 shows the polarization against electric field (P–E) hysteresis loops of a series of ceramics with different Ti contents within the rhombohedral phase of PZT. While ceramics with 6% Ti content (PZT06) present an ordinary squarelike loop (figure 3(a)), an increase of the Ti level (PZT12 and PZT40) results in double loops with almost no remanent polarization (figures 3(b) and (c)). When the composition approaches the rhombohedral–tetragonal morphotropic phase boundary (PZT45) the remanent polarization increases (figure 3(d)). These results corroborate the previously observed evolution of the hysteresis loops in

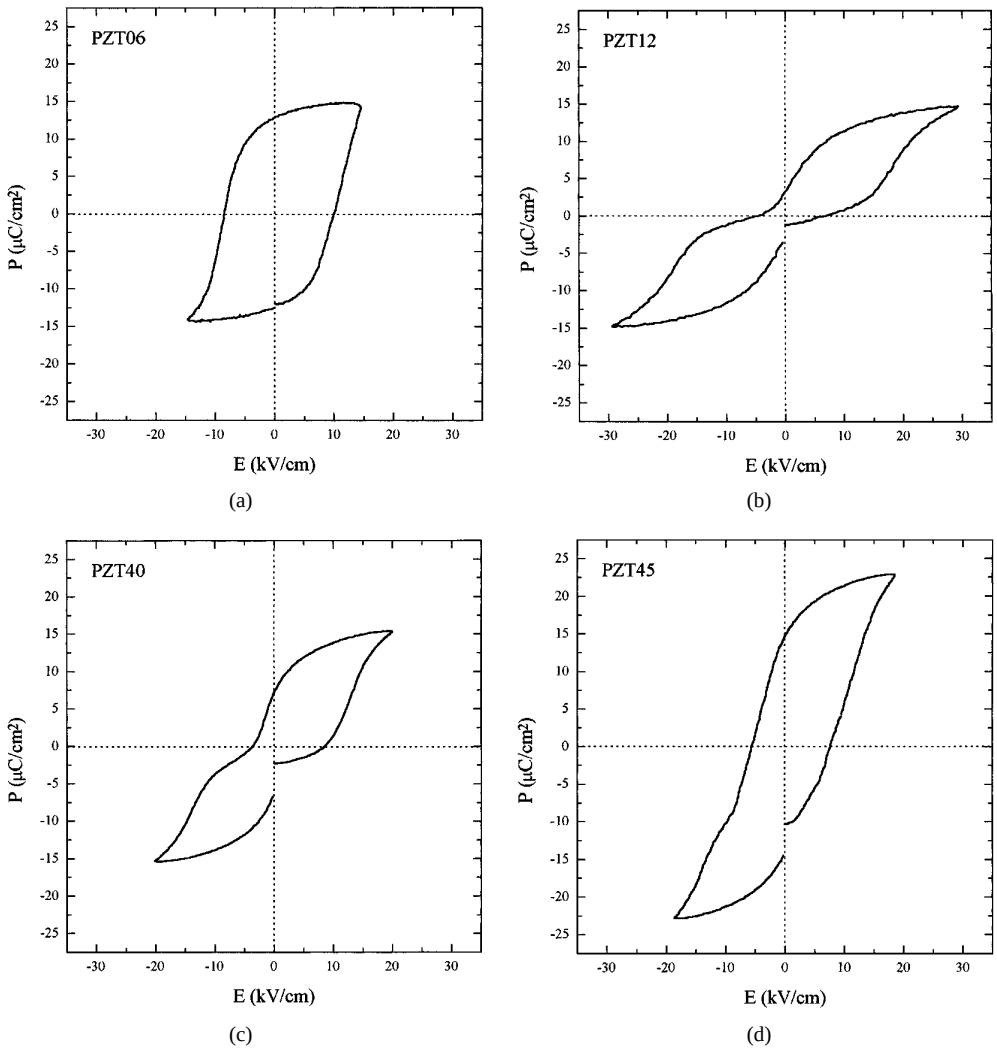

Figure 3. Room temperature polarization against electric field (P–E) curves. (a) PZT06. (b) PZT12. (c) PZT40. (d) PZT45.

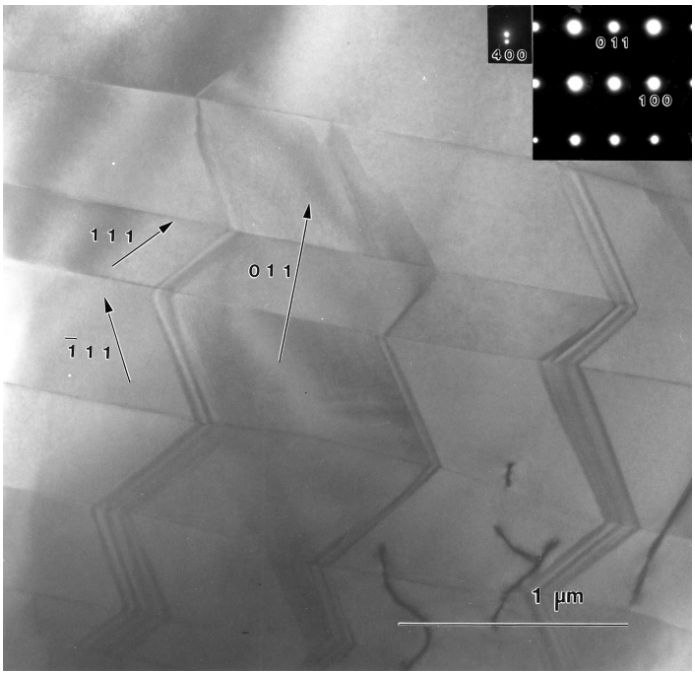

Figure 4. TEM bright field micrograph of PZT06 ceramics showing a herringbone-like ferroelectric domain configuration, viewed along [0$\bar{1}$1]. The (400) reflection is enlarged to show the splitting of the spots.

rhombohedral PZT [8], which develops constriction of the polarization state as the Ti content increases and this effect only starts to disappear for compositions close to the transition to the tetragonal phase. An attempt to 'de-age' a PZT12 ceramic was carried out, by annealing the sample for 3 hours at 500 °C. After cooling to room temperature, the sample was prepared with fresh electrodes and a hysteresis loop re-measured within hours of cooling to room temperature. It was observed that the double-loop character was essentially unchanged from that recorded prior to the 'de-ageing' treatment.

The ferroelectric domain configurations of the same ceramics have been characterized by TEM. Selected images are shown in figures 4 to 9. Generally, the observed domains are quite mobile and unstable under the influence of the electron beam and typically their sizes go from 100 to 800 nm in width. The domain walls observed in this work are mainly {110}-type walls. It has been reported that the surface energy of a twin boundary on a {100} plane is three times of that on a {110} plane, and, therefore, they are less likely to occur [19].

Figures 4 and 5 present micrographs of the domain configurations observed in PZT06 ceramics. Figure 4 shows a herringbone-like domain configuration, similar to the ones observed and modelled for $BaTiO_3$ [22]. The domains are viewed along [0$\bar{1}$1], and the main crystallographic directions are labelled. The long lines are identified as traces of (011) walls, while the zigzag lines showing fringes correspond to (110), (101), ($\bar{1}\bar{1}$0) and ($\bar{1}$01) walls (see figure 2(a) for interpretation). The electron diffraction pattern from this region shows splitting in the high order diffraction reflections, as in the (400) reflection enlarged in the inset. The splitting is along [011], which means that it is the result of the presence of (011) twin planes corresponding to ferroelectric domain walls. As the other domain walls present are inclined to

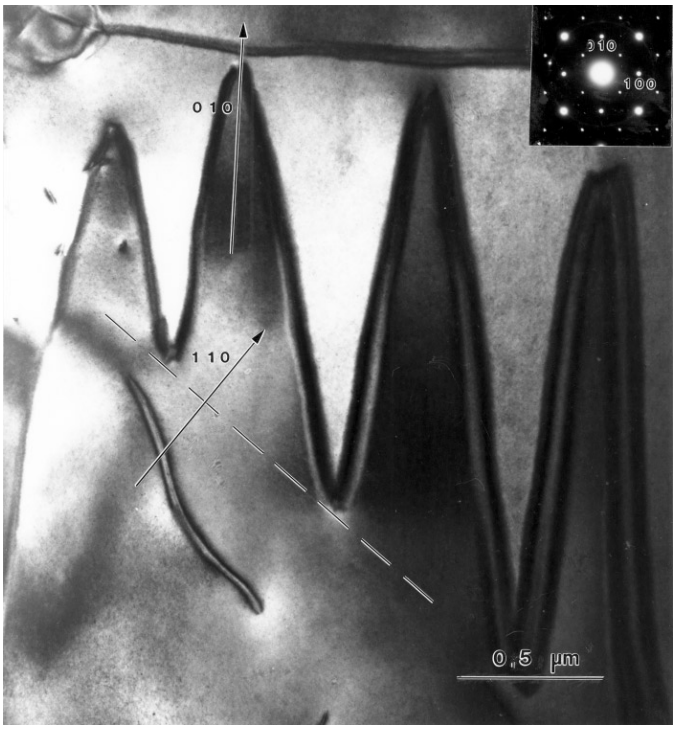

(a)

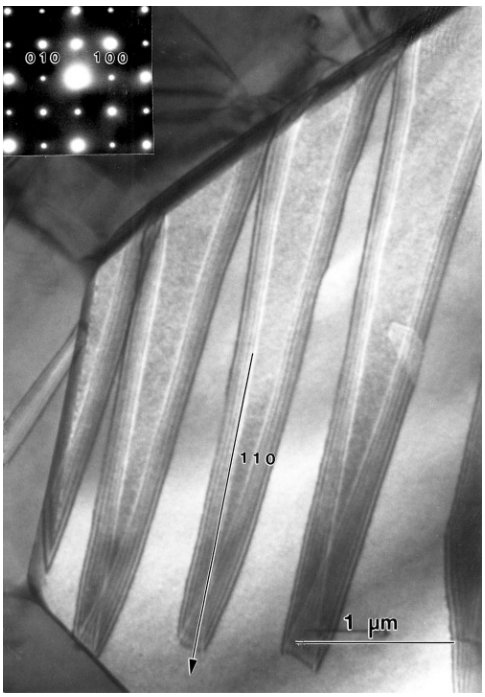

(b)

Figure 5. BF micrographs of PZT06 ceramics showing misoriented ferroelectric domain walls and wedge-shaped domains, viewed along [001].

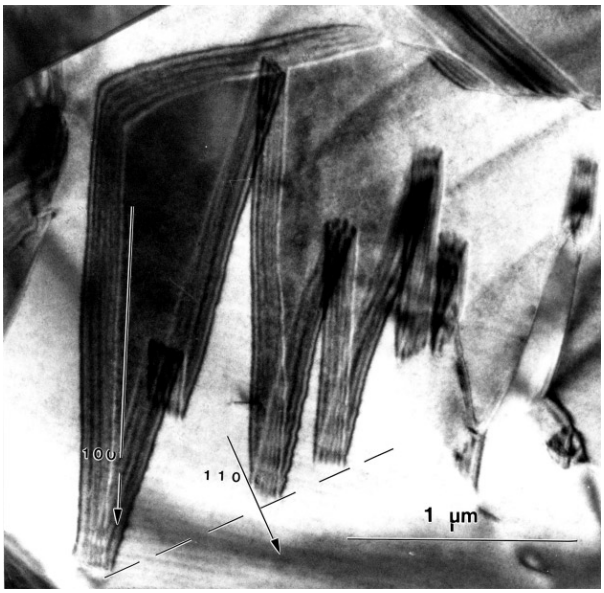

(a)

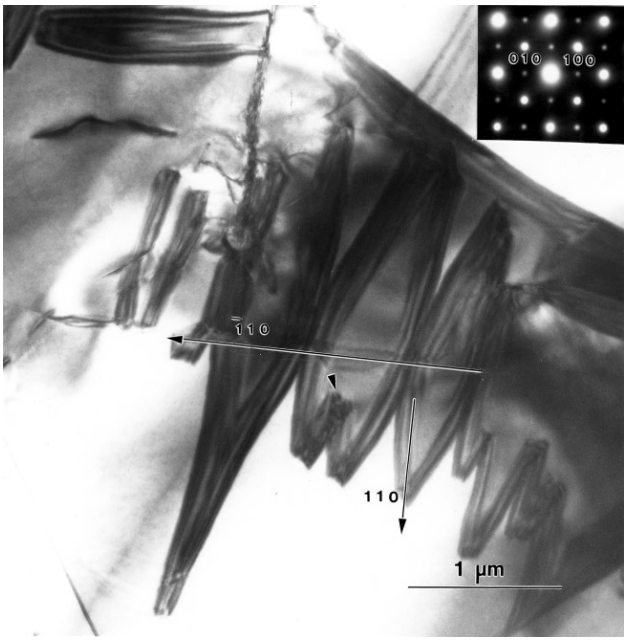

(b)

Figure 6. BF micrographs of PZT12 showing wedge-shaped domains, viewed along [001].

the electron beam, no significant splittings along other directions are observed. These domains show all the characteristics of the predicted configuration of complex bands of twins resulting from the paraelectric–ferroelectric transition.

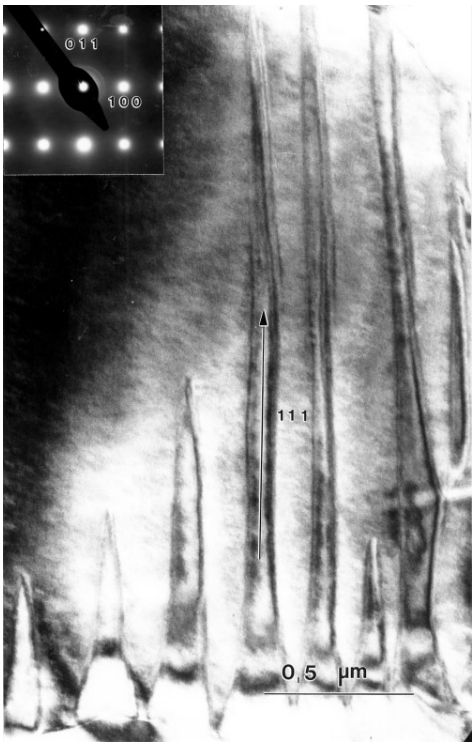

Figure 7. BF micrograph of PZT40 showing a typical ferroelectric domain configuration viewed along [0$\bar{1}$1].

The herringbone-like configuration of domains is not the only type observed in PZT06 ceramics. On the contrary, wedge-shaped domains, like the ones shown in figure 5(a), are in fact the most commonly observed configuration. The wedges point in a [010] direction and go from a (010) wall at the top to an invisible line at the bottom (marked with a dashed line on the micrograph), which corresponds to a (110) plane. The domains are viewed along the [001] zone axis, and, as shown in figure 1(a), traces of inclined (101) walls are expected to appear as parallel lines along the [010] direction. Instead, we have wedges pointing in that direction, which can be considered as two sets of (101) walls slightly misoriented in different directions which intersect at some point. Superlattice reflections appearing in the diffraction patterns are discussed in a previous paper [25].

It has to be pointed out that not all the wedge-shaped domains observed when viewing along this zone axis point in [100] or [010] directions. Figure 5(b) shows an example of wedges pointing in a direction closer to [110]. In this case, the domain configuration is produced by sets of misoriented (110) walls. Not only do these walls not follow the expected directions, but also they are inclined to the electron beam and show fringes. This shows that the tilt of the walls occurs in three dimensions. As in figure 5(a), the domain walls start at the grain boundary at the bottom and terminate inside the grain so that the tips of the wedges follow the trace of a (110) plane.

Increase of the Ti content leads to the domain configurations shown in figures 6 and 7 for PZT12 and PZT40, respectively. Series of wedges pointing in [100] directions are again observed in PZT12 ceramics (figure 6(a); grains are viewed along [001]). This is a similar

Figure 8. BF micrograph showing the mixture of two different types of domain configuration in PZT45, viewed along [001]. The insets show the selected-area diffraction patterns of the region of domain bands (top) and of wedge-shaped domains (bottom). The (500) reflection is enlarged to show the splitting of the spot.

situation to figure 5(a) for PZT06, and, similar to the previous case, the walls can be identified as sets of misoriented (011) planes. Some walls also terminate in a definite line that corresponds to the [110] direction. However, most of the terminations of the wedges do not follow any particular pattern. The same behaviour can be found for wedges pointing in a direction close to [110] (figure 6(b)). In this case the sets of misoriented (110) walls are remarkably curved as well. The three domains in the middle are two wedges joining in a straight line, which is a trace of a (110) wall. The wedges at the top finish at the grain boundary, while for the terminations at the bottom we cannot find any associated microstructural feature. A particular case is the domain labelled with an arrow, where the wedge finishes in two tips, instead of one. We call this bifurcation of a domain.

Figure 7 shows a configuration for PZT40 that consists of parallel bands. The walls can be identified as $(\bar{1}10)$ or (101) walls (grains are viewed along $[0\bar{1}1]$, see figure 2(a) for

Figure 9. BF micrograph showing the complex domain configuration of PZT45 ceramics (grain viewed along [0$\bar{1}$1]).

interpretation). They started growing from the grain boundary, but some of them did not reach the other side of the grain and, unlike PZT06, they did not follow any particular pattern in the position of their terminations. The facts that PZT12 and 40 exhibit domain walls whose terminations do not follow any pattern, and that there is occasional domain bifurcation, can be considered as distinctive features of these domain configurations.

Moving to compositions closer to the phase transition to the tetragonal phase (PZT45), a configuration of simple parallel bands of domains is more often observed, like the example shown at the top of figure 8. The domain walls correspond to the predicted (110) twinning planes. However they present bifurcation at some points close to the edges of the domains (marked with arrows on the micrograph). In the same grain at the bottom of the figure, there are areas showing wedge-shaped domains. They point in a [010] direction, and can therefore be identified as misoriented (101) walls. Selected-area electron diffraction patterns were obtained from the region of parallel bands (inset at the top) and on the wedge-shaped domains (inset at the

bottom). In these diffraction patterns the splitting of the electron diffraction spots perpendicular to the (110) walls produced by the parallel bands of domains is easily seen, even for low index reflections. However, the splitting perpendicular to (101) resulting from the wedge-shaped domains is smaller, and therefore can only be seen in higher order reflections. This difference can be easily seen in the enlarged (500) reflection. The large splitting obtained in the diffraction pattern from the banded region does not seem characteristic of the rhombohedral phase, which usually shows smaller splitting of the electron diffraction spots, like the one shown in figure 4 for PZT06. This seems to indicate the presence of another phase in these grains, like the more Ti-rich tetragonal phase which produces a larger splitting than the rhombohedral phase due to the larger differences in the lattice spacing both sides of the 90° domain walls.

Similar characteristics to the ones found for PZT12 and 40 are still observed for PZT45 (figure 9): walls that terminate without following any pattern (top of figure 9) or curved walls, together with herringbone-like configurations: (110), (101), $(\bar{1}\bar{1}0)$ and $(\bar{1}01)$ walls meeting in a (011) wall (marked with a dashed line).

5. Discussion

The work presented here has shown for the first time that there is a marked systematic variation in the character of the domain walls as the composition progresses across the rhombohedral region of the lead zirconate–lead titanate phase diagram from PZT06 to PZT45. While PZT06 shows the typical herringbone-like configuration mixed with wedge-shaped domains with misoriented {110} walls, the distinctive features of PZT12 and PZT40 domains are the occasional bifurcation and the fact that in general the domain wall terminations do not follow any particular pattern. For high Ti contents, the proximity to the phase transition and to the tetragonal phase, which does not show wedge-shaped domains [17], leads the ferroelectric domain arrangements to favour again the appearance of herringbone-like configurations. However, some of the characteristics described above for PZT12 and 40 are still present.

The domain configurations observed in these ceramics show in most cases walls which do not correspond exactly to twinning planes. As a result of these deviations, the walls tend to form wedges, instead of the expected bands of parallel domains. Similar wedge-shaped domains have been reported before in $BaTiO_3$ [13]. TEM studies of ferroelectric domains in ceramics often report wedge domains as small deviations of the orientation near the terminations of the walls, which can be explained by the presence of local stress produced by grain boundaries or other domain walls. However, in the rhombohedral PZT ceramics studied here the misoriented walls do not appear to be localized near other microstructural features in the crystal, but they extend across the grains. Therefore, we consider this as a characteristic feature of these compositions.

It has been suggested that there exist local random oxygen octahedral rotations in the rhombohedral phase [5], which produce strains and then disrupt the long-range polar order. If this were to be the case, then we can postulate the existence of localized regions of stress inside the grains where the values of the dielectric polarization are lower than average. As the domain walls are created to minimize the elastic and electric stresses associated with the transition from the paraelectric to the ferroelectric state, these variations in stress can affect the positions of the domain walls. This probably causes the observed deviations from the predicted twinning planes and the curved walls. Most likely, it is the fact that they do not correspond to crystallographic planes (simplest structure and minimum energy in ideal case) which makes them more mobile under the electron beam than parallel-walled domains, as the observations show.

There is clearly a question as to whether the evolution in the domain patterns as the composition moves across the rhombohedral phase region, as reported here, is connected to the observed change in the character of the ferroelectric hysteresis loops (i.e. the observed change from square to double and back to square again moving from PZT06 through PZT12 and 40 to PZT45). At first sight, it might be considered that the double loops for PZT12 and PZT40 are caused by the pinning of the ferroelectric domains by the migration of charged defects under the action of the depolarization field. This has been postulated as the reason for the appearance of similar loops in the commercial 'hard' PZT ceramics, which are acceptor doped [11]. Indeed, the existence of Pb vacancies in the undoped PZT ceramics studied here would be expected to act as acceptor centres and could plausibly lead to a similar effect. There are two problems with this interpretation of the double loops we observed in these compositions. The first is that the double-loop effect in the acceptor doped PZT can be reversed by thermal annealing (or de-ageing). Such de-aged ceramics show normal loops until they have been left for some considerable time (many hours at room temperature), when the double-loop character progressively reasserts itself. A de-ageing experiment carried out on PZT12 showed that after thermal annealing, this specimen still showed a double-loop character, essentially unchanged. The second reason for rejecting this ageing model is, perhaps, the most obvious one. This is that, if the double loops in PZT12 and PZT40 are caused by the migration of charged defects pinning the domain walls, why is the effect not seen in PZT06 and PZT45, which are very close in composition to these? It would seem that the simplest explanation for the observed double loops is that PZT12 and PZT40, which exhibit double loops, sit well within the $F_{R(LT)}$ phase region, while the PZT06 and PZT45 compositions, which do not, are respectively at the low-Ti and high-Ti edges of it. We should, therefore, look for explanations for the hysteresis loop and domain characters which are intrinsic to the crystal structure and not extrinsic factors introduced by defects.

Ceramics showing normal square-type (single) hysteresis loops, like PZT06, also exhibit microstructures where ferroelectric domains start and finish in the grain boundaries or domain walls. It seems that variations in this basic configuration favour the occurrence of double hysteresis loops (PZT12 and 40). When the compositions are close to the rhombohedral–tetragonal morphotropic phase boundary (PZT45), regions with tetragonal structure showing bands of parallel domains appear, mixed with regions of the rhombohedral phase which still exhibit wedge-shaped domains. The remanent polarization and normal square character seems to be almost regained.

If we look for an explanation for the double-loop character in terms of the oxygen octahedral tilting of the $F_{R(LT)}$ phase (rhombohedral at low temperature), we can first note that the polarization in the tilted rhombohedral compositions is dependent on the magnitude of the octahedral tilt angle [26]. This is clearly shown by the step-decrease in the spontaneous polarization of $PbZr_{0.91}Ti_{0.09}O_3$ on heating through the $F_{R(HT)}$ (rhombohedral at high temperature) to $F_{R(LT)}$ phase transition [27]. If we consider the cycling of the structure through the hysteresis loop while in the $F_{R(LT)}$ phase, it is possible that the inversion of the octahedral tilts (which would involve switching their rotational sense) is more difficult to switch than the spontaneous polarization. It is thus possible to postulate a situation where the octahedral tilts are not inverted during the hysteresis loop cycle, reducing the switchable part of the spontaneous polarization. If this were the case, then the polarization component due to the tilting would not be switched and would establish a pattern of polarization in the crystal which would reflect the domain structure established on cooling through the $F_{R(HT)}$ to $F_{R(LT)}$ phase transition. This would tend to re-establish the original domain pattern when the applied field is removed, and the net spontaneous polarization would have a tendency to reduce to zero, giving place to the observed double-loop behaviour. Hence, the ferroelectric domains

would have a natural tendency to become 'pinned' by the pattern of rotational tilts within the grains. This pattern within any one grain would be expected to be highly dependent on the grain's elastic stress state as the octahedral tilt transition is ferroelastic. This would account for the observation that the domains in PZT12 do not start at the grain or domain boundaries. This transition is from one ferroelectric phase $F_{R(HT)}$ (rhombohedral at high temperature) to another ferroelectric phase $F_{R(LT)}$ (rhombohedral at low temperature). Therefore, grains would have developed a ferroelectric domain configuration in $F_{R(HT)}$, which is disrupted when going through this phase transition. Traces of nucleation of new domain walls on a previous domain configuration (bifurcation) have been observed and we believe that this supports the argument presented above.

Looking at the phase diagram of PZT, this effect would be expected to be at its greatest with those compositions whose $F_{R(HT)}$ to $F_{R(LT)}$ transition temperature was the highest, and so would disappear at each end of the $F_{R(LT)}$ phase region, as observed (PZT06 and PZT45). Furthermore, the effect would not be reversible by attempts to de-age the specimens. At the moment this model is, necessarily, a postulate, and further work would be required to verify it. We suggest that structural studies as neutron diffraction with Rietveld refinement while under hysteretic cycling would be informative. This could be achieved by using a pulsed neutron source with the frequency and phase of the hysteresis drive locked to the source. This would permit the relative signs and magnitudes of cationic displacements and octahedral rotations to be observed at different points around the loop. Further, if the postulated model is correct, we might expect the shapes of the double loops to be frequency dependent, probably opening up at very low frequency. We therefore suggest that the frequency dependence of the hysteresis loops in these compositions be investigated.

6. Conclusions

A TEM study of the ferroelectric domain configurations of rhombohedral PZT ceramics has been carried out, followed by a complete analysis of the nature of the domain walls, based on the predicted twinning planes for the formation of domains in the rhombohedral system. As a result, a systematic variation of the characteristics of the domain walls as the compositions moves across the rhombohedral region is reported for the first time. Occasional bifurcation and domain walls whose terminations do not follow any particular pattern, and the tendency to develop herringbone-like configurations at each end of the rhombohedral phase, are the main features of the evolution observed. In general, the domains in these compositions are wedge shaped due to the fact that domain walls are misoriented with respect to the predicted twinning planes. A plausible explanation for this characteristic feature may be the existence of local random strains within the grains due to the oxygen octahedral rotations within this phase.

Comparing the evolution of the domain configuration and the changes in the character of the hysteresis behaviour, we observe that while ceramics showing normal single loops exhibit ferroelectric domains which start and finish in grain boundaries or domain walls, deviations from this configuration seems to favour the occurrence of double loops. Looking for an explanation which is intrinsic to the crystal structure of these compositions, we find that the tilting state of the oxygen octahedra corresponding to the low temperature rhombohedral $F_{R(LT)}$ phase could account for the characteristic features of the domain configurations and the appearance of double hysteresis loops. According to this model, the effect would disappear for compositions at each end of the $F_{R(LT)}$ phase, as observed in this work. Further structural work to study the postulated model is suggested.

Acknowledgments

The authors wish to thank Dr D L Corker for useful discussions and Mr A M Stallard (Cranfield University) for ceramic preparation. Professor R W Whatmore gratefully acknowledges the financial support of the Royal Academy of Engineering. This work was funded by the Engineering and Physical Sciences Research Council (EPSRC).

References

[1] Berlincourt D. 1992 *J. Acoust. Soc. Am.* **91** 3034–40
[2] Whatmore R W 1986 *Rep. Prog. Phys.* **49** 1335–86
[3] Harris J O Jr, Cutler R P and Dulleck G R 1986 *Proc. 6th IEEE Int. Symp. on Applications of Ferroelectrics (Bethlehem, 1986)* pp 57–61
[4] Arlt G, Hennings D and de With G 1985 *J. Appl. Phys.* **58** 1619–25
[5] Jaffe B, Cook W R and Jaffe H 1971 *Piezoelectric Ceramics* (London: Academic)
[6] Jonker G H 1972 *J. Am. Ceram. Soc.* **55** 57–8
[7] Sawaguchi E and Charters M L 1959 *J. Am. Ceram. Soc.* **42** 157–64
[8] Dai X, Xu Z and Viehland D 1995 *J. Am. Ceram. Soc.* **78** 2815–27
[9] Bradt R C and Ansell G S 1969 *J. Am. Ceram. Soc.* **52** 192–9
[10] Dederichs H and Arlt G 1986 *Ferroelectrics* **68** 281–92
[11] Carl K and Härdtl K H 1978 *Ferroelectrics* **17** 473–86
[12] Ikegami S and Ueda I 1967 *J. Phys. Soc. Japan* **22** 725–34
[13] Tanaka M and Honjo G 1964 *J. Phys. Soc. Japan* **19** 954–70
[14] Hu Y H, Chan H M, Wen Z X and Harmer M P 1986 *J. Am. Ceram. Soc.* **69** 594–602
[15] Demczyk B G, Rai R S and Thomas G 1990 *J. Am. Ceram. Soc.* **73** 615–20
[16] Lee Y Y, Wu L and Chang J S 1994 *Ceram. Int.* **20** 117–24
[17] Goo E K W, Mishra R K and Thomas G 1981 *J. Appl. Phys.* **52** 2940–3
[18] Cao W and Randall C A 1996 *J. Phys. Chem. Sol.* **57** 1499–1505
[19] Randall C A, Barber D J and Whatmore R W 1987 *J. Mater. Sci.* **22** 925–31
[20] Fousek J and Janovec V 1969 *J. Appl. Phys.* **40** 135–42
[21] Arlt G 1990 *J. Mater. Sci.* **25** 2655–66
[22] Arlt G and Sasko P 1980 *J. Appl. Phys.* **51** 4956–60
[23] Verwerft M, van Tendeloo G, van Landuyt J and Amelinckx S 1989 *Ferroelectrics* **97** 5–17
[24] de Ridder R, van Landuyt J. Gevers R and Amelinckx S 1968 *Phys. Status Solidi* **30** 797–815
[25] Ricote J, Corker D L, Whatmore R W, Impey S A, Glazer A M, Dec J and Roleder K 1998 *J. Phys.: Condens. Matter* **10** 1767–86
[26] Haleman T R, Haun M J, Cross L E and Newnham R E 1985 *Ferroelectrics* **62** 149–65
[27] Clarke R, Glazer A M, Ainger F W, Appleby D, Poole N J and Porter S G 1976 *Ferroelectrics* **11** 359–64